THE JOURNAL OF PHYSICAL CHEMISTRY B
A JOURNAL OF THE AMERICAN CHEMICAL SOCIETY

pubs.acs.org/JPCB

Article

Dual Role of Anionic Lipids in Amyloid Aggregation

Meenal Jain and Silvina Matysiak*

Cite This: J. Phys. Chem. B 2024, 128, 10831−10840

Read Online

ACCESS | Metrics & More | Article Recommendations | Supporting Information

ABSTRACT: Neurodegenerative diseases, such as Alzheimer's, Parkinson's, and Huntington's, affect millions worldwide and share a common feature: the aggregation of intrinsically disordered proteins into toxic oligomers that interact with cell membranes. In Alzheimer's disease (AD), amyloid-beta (Aβ) peptides accumulate and bind to plasma membranes, potentially disrupting cellular function. The complex interplay between amyloidogenic peptides and lipid membranes, particularly the role of anionic lipids, is crucial in disease pathogenesis but challenging to characterize experimentally. The literature presents conflicting results on the influence of anionic lipids on peptide aggregation kinetics, highlighting a knowledge gap. To address this, we used coarse-grained molecular dynamics (CG-MD) simulations to study interactions between a model amyloidogenic peptide, amyloid-β's $K_{16}LVFFAE_{22}$ fragment ($A\beta_{16-22}$), and mixed lipid bilayers. We used phosphatidylserine (PS) and phosphatidylcholine (PC) as representative anionic and zwitterionic lipids, respectively, examining the mixed bilayer compositions of 0% PS−100% PC, 10% PS−90% PC, and 30% PS-70% PC. Our simulations revealed that membranes enriched in anionic lipids enhance peptide adsorption and interaction kinetics. The aggregation dynamics was modulated by two competing factors: increased local peptide concentration near negatively charged membranes, which promoted aggregation, and peptide−lipid interactions, which slowed it down. Higher percentages of anionic lipids led to smaller and more ordered aggregates and enhanced lipid demixing, leading to the formation of PS clusters. These findings contribute to understanding membrane-mediated peptide aggregation in neurodegenerative disorders, potentially guiding new therapeutic strategies targeting the early stages of protein aggregation in various neurodegenerative diseases.

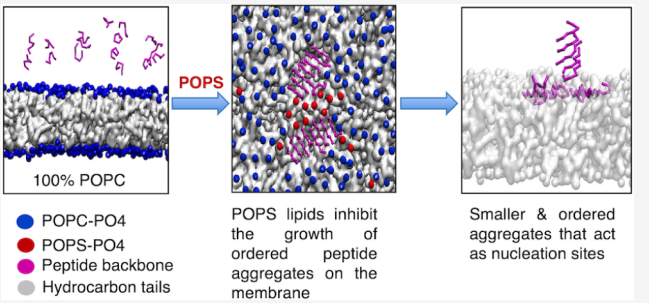

INTRODUCTION

Neurodegenerative disorders, such as Alzheimer's, Parkinson's, Huntington's, and type 2 diabetes, affect hundreds of millions of people worldwide, with Alzheimer's disease (AD) alone affecting approximately 45 million individuals worldwide and being the fifth leading cause of death globally.[1,2] These conditions are characterized by the aggregation of intrinsically disordered proteins (IDPs), such as amyloid-beta (Aβ), alpha-synuclein, huntingtin, and human islet amyloid polypeptide.[1,2] Self-assembly of these peptides form oligomeric and fibrillar aggregates, with the consensus that oligomers are the primary toxic species.[3] Notably, the oligomeric aggregates for all of these disorders share a common structural and evolutionary pathway when interacting with cell membranes. This resemblance in oligomeric behavior facilitates the extrapolation of the mechanisms of peptide binding/aggregation on the membrane and the subsequent changes in membrane structure to most of these neurodegenerative disorders.[1]

In particular, AD is characterized by extracellular senile plaques and intracellular neurofibrillary tangles with the accumulation of amyloid-beta (Aβ) peptides playing a crucial role in its pathogenesis. These peptides, cleaved from the transmembrane amyloid precursor protein (APP) by β- and γ-secretase complexes, possess an innate affinity for cellular membranes due to their origin.[4] This affinity is pivotal in AD pathology, as Aβ undergoes a critical structural transition from disordered monomers to ordered oligomers upon membrane binding.[1] The peptide−lipid interactions not only facilitate this transition but also contribute to the disruption of plasma membrane integrity, a process postulated to be a potential mechanism of neurotoxicity in AD.[1] Understanding this peptide−lipid dynamics is crucial as they drive the progression of Alzheimer's disease, highlighting an area for further research and potential therapeutic interventions in combating this neurodegenerative disorder.

The experimental literature presents conflicting results regarding the influence of anionic lipid composition on the aggregation kinetics of Aβ and other neurodegenerative peptides, highlighting a gap in our understanding of peptide-lipid interactions. Some studies, such as those by Sabaté et al. and Sanguanini et al., report that increasing the proportion of

Received: August 21, 2024
Revised: October 17, 2024
Accepted: October 21, 2024
Published: October 25, 2024

anionic lipids in mixed zwitterionic/anionic lipid vesicles leads to delayed aggregation kinetics.[5,6] Conversely, works by Niu et al. and Lv et al. demonstrate an acceleration of aggregation kinetics as the negative charge of lipid vesicles increases, compared to aggregation in solution.[7,8] These apparent discrepancies can be attributed to several factors: (1) variations in lipid to peptide ratios, which affect the concentration of peptides relative to lipids;[9] (2) differences in the biophysical models of membranes used;[10] and (3) various sample preparations and experimental techniques used to monitor the aggregation kinetics.[10] These conflicting results highlight the complexity of Aβ−lipid interactions and the need for a more comprehensive understanding of the underlying mechanisms.

The transient and soluble nature of Aβ oligomers[11] poses significant experimental challenges for capturing molecular-level details. To address this limitation, computational studies, particularly molecular dynamics (MD) simulations, are extensively used.[12] Although atomistic MD simulations of peptide aggregation are constrained by high computational costs and sampling issues, coarse-grained (CG) MD offers a solution by grouping chemically similar atoms into CG beads, smoothening the free-energy landscape of peptide aggregation.[13] The combination of experimental techniques and CG-MD simulations enables the exploration of extended spatio-temporal scales, providing crucial insights into peptide aggregation on lipid bilayer membrane that are otherwise challenging to obtain through experimental methods alone.[12]

Cellular membranes exhibit complex, asymmetric lipid compositions, with phosphatidylcholines (PCs) dominating the outer leaflet and phosphatidylserines (PSs) typically confined to the inner leaflet of healthy cells.[14,15] However, cellular dysfunction, often associated with neurodegenerative diseases, can cause PS externalization, creating a favorable environment for amyloid peptide aggregation.[16] Our previous work with pure PS and PC membranes revealed more ordered peptide aggregates and lower cumulative aggregation rates on PS membranes, highlighting the significant impact of membrane composition on Aβ_{16-22} interaction kinetics and dynamics.[17] Given that plasma membranes are lipid mixtures rather than pure compositions, mixed PC/PS lipid bilayers serve as more realistic models for the outer leaflet with exposed PS.[18] In this study, we employ mixed PC/PS lipid bilayers to investigate the influence of anionic lipid composition on Aβ_{16-22} binding and aggregation on plasma membranes as well as the reciprocal effects of these interactions. This approach, supported by various experimental studies and MD simulations, offers insights into the complex interplay between lipid composition and amyloid peptide behavior in the context of neurodegenerative diseases.[5,7,18,19]

In this study, we employ CG-MD simulations to investigate the interactions between Aβ_{16-22} (K−L−V−F−F−A−E) peptides and model lipid bilayer membranes. This seven-residue segment represents the shortest fragment of the Aβ peptide capable of independently forming fibrils, making it a useful model for studying the behavior of amyloidogenic peptides.[20] Experimental studies have examined the interactions of similar short Aβ fragments, such as Aβ_{16-28}, with lipid membranes.[21] We used a modified version of water-explicit polarizable PROtein model (WEPROM)[22] to model the peptides and the water-explicit polarizable MEMbrane (WEPMEM)[23] model for the lipids. Both of them are compatible with Yesylevskyy et al.'s polarizable CG water model,[24] which we have used to model water. To gain a molecular-level understanding of how the composition of anionic lipids affects Aβ_{16-22} binding, aggregation, and subsequent membrane disruption, we examine three distinct bilayer compositions of anionic POPS (1-palmitoyl-2-oleoyl-*sn*-glycero-3-phospho-L-serine) and zwitterionic-POPC (1-palmitoyl-2-oleoyl-*sn*-glycero-3-phosphocholine): 0% POPS−100% POPC, 10% POPS−90% POPC, and 30% POPS−70% POPC. While 30% PS is higher than typical physiological levels, similar percentages have been used in previous experimental and computational studies, allowing us to observe more pronounced effects.[5,19,25] By systematically varying membrane composition, we tried to unravel the complex interplay between Aβ_{16-22} peptides and lipid membrane compositions. In our simulations of binding of Aβ_{16-22} to mixed membranes, we observe enhanced membrane adsorption and smaller, more ordered aggregates with higher percentages of PS. Also, we see PS lipids (a) clustering around Aβ_{16-22} peptides and (b) forming PS clusters (regions of high negative charge density). Our findings offer a potential explanation for the discrepancies in experimental literature regarding the impact of anionic lipid composition on Aβ_{16-22} aggregation kinetics in neurodegenerative diseases. By providing valuable insights into the mechanisms of peptide−membrane interactions, we provide a framework to reconcile contradictory results observed in various experimental studies. These insights may guide the development of novel therapeutic strategies targeting the early stages of amyloid aggregation in the context of Alzheimer's and related neurodegenerative disorders.

METHODS

CG Model Details. Aβ_{16-22} (K_{16}LVFFAE_{22}) was modeled using a modified version of CG WEPROM force field,[22] which has been previously employed to investigate the aggregation behavior of peptides under various conditions, including at hydrophobic−hydrophilic interfaces,[26] across different concentrations of glucose,[27] and in the presence of aggregation inhibiting macromolecules, such as chitosan.[28] For details on the modifications made to the WEPROM force field, please refer to Sahoo et al.[17] The lipids POPC and POPS were modeled using the CG WEPMEM force field.[23] This force field has previously been used to study calcium-assisted lipid demixing,[29] peptide aggregation in membranes composed of 100% POPC or 100% POPS,[17] and in membranes with varying curvatures.[30]

The beads in the CG models for peptide and lipids are broadly classified into polar, hydrophobic, and charged categories, each with a specific set of interactions. While our models retain most bead definitions and interaction levels of MARTINI,[31,32] there are two notable differences. First, the polar beads incorporate a dipole made up of Drude-like oscillating charges, which couple the environmental fluctuations to the macromolecule's structure through electrostatics. The van der Waals interactions between these polar beads and other charged and polar beads were scaled down from MARTINI values to compensate for the added electrostatics through this dynamic dipole. Second, the interactions between hydrophobic and solvent beads were reduced from MARTINI values to facilitate the folding of peptides into β-sheets.[23]

Figures S1 and S2 illustrate the CG models for peptides and lipids, respectively. For peptides, we represent each amino acid with one backbone (BB) bead and specific side chain beads (S1/S2). The backbone was modeled with polar beads to capture the dipole moment associated with peptide bonds. The side chains were tailored to each amino acid type: phenylalanine was represented by two hydrophobic beads, while valine and leucine

https://doi.org/10.1021/acs.jpcb.4c05636
J. Phys. Chem. B 2024, 128, 10831−10840

each had one hydrophobic bead. The flanking amino acids lysine and glutamate were modeled with one hydrophobic and one charged bead each. For lipid molecules, the headgroups for POPC was modeled with two charged beads: one for choline (NC3) and one for phosphate (PO4), while that for POPS consisted of one polar bead for serine (CNO) and one charged bead for phosphate (PO4). The glycerol esters for both lipids were represented by polar beads (GL1 and GL2), while the oleoyl and palmitoyl tails were modeled with five and four hydrophobic beads, respectively.[23] The presence of structural polarization (via dummy charges) at the peptide-backbone and lipid-headgroup facilitates the study of peptide−lipid interactions.

We used the polarizable MARTINI water model[24] to represent CG water and standard MARTINI monovalent ions to neutralize the system, as both are compatible with our lipid and peptide models. Details regarding the bonded and nonbonded interaction parameters for these models can be found in Ganesan and Matysiak[22] and Sahoo et al.[17] Table S1 and Figure S3 provide the CG bead types and Lennard−Jones interaction parameters between all bead types used in this study.

Simulation Setup. To investigate the effects of lipid composition on Aβ_{16-22} adsorption and aggregation, three composite lipid bilayer membranes containing 0%, 10%, and 30% POPS, complemented by 100%, 90%, and 70% POPC, respectively, were constructed using the insane program.[33] Each simulation system consisted of a lipid bilayer membrane containing 338 lipid molecules with the necessary counterions to neutralize the negative charges of POPS lipids. We solvated the membrane with approximately 12,800 CG water beads, maintaining a water-to-lipid ratio of 20:1. To mimic the outer membrane of a small unilamellar vesicle (SUV), the lipid bilayer membranes were simulated at surface tension values corresponding to an area-per-lipid (APL) of 95 Å^2. This specific area-per-lipid metric was obtained from the WEPMEM simulation of an SUV with a diameter of 13.4 nm, containing 877 lipids and 61,113 coarse-grained water molecules, as reported by Sahoo et al.[17] Furthermore, membranes with varied percentages of POPS exhibited distinct surface tension values corresponding to an APL of 95 Å^2, as shown in Table S3. These values were determined through an APL versus surface tension plot (Figure S4), which was generated from 100 ns simulations performed at multiple surface tension values across different PS percentages. The details about these simulations can be found in Supporting Information.

Each composite lipid bilayer membrane was initially energy minimized and equilibrated by using the NPT ensemble for 100 ns at a surface tension corresponding to an area-per-lipid (APL) of 95 Å^2. After obtaining the desired APL, the bilayer was transferred to a periodic box with dimensions of 12.5 × 12.5 × 13 nm^3. Water molecules and necessary counterions were added to neutralize the system, which was energy minimized and further equilibrated with restraints on the phosphate (PO4) groups for 5 ns. After the creation of an equilibrated bilayer with an APL of 95 Å^2, 16 Aβ_{16-22} peptides were positioned within the periodic box, about 4 nm away from both surfaces of the bilayer. This configuration resulted in a peptide concentration of 13.1 mM with a lipid:peptide ratio of 10:1. This ratio has been previously investigated in small (Aβ_{25-35}) peptide-membrane experiments.[34] We instituted a hardcore repulsion ($4\varepsilon\sigma^6$ = 0 kJ·mol^{-1}·nm^{-6} and $4\varepsilon\sigma^{12}$ = 0.00247 kJ·mol^{-1}·nm^{-12}) between the lower leaflet lipid (NC3, PO4, GL1, GL2, CNO) beads and the peptide beads. Such repulsive potentials do not affect peptide aggregation and adsorption properties on the opposite layer, as shown by previous simulations.[17,30] The entire system was then energy minimized and re-equilibrated for 50 ns, with positional restraints applied to BB beads of F19 in the peptides and PO4 beads in the lipids. After releasing the restraints, a production run of 3 μs was carried out using the simulation parameters described below.

All simulations were performed on GROMACS 2019.4. The temperature was maintained at 300 K using a Nosé−Hoover thermostat[35] with a time constant of 1 ps. Pressure control was achieved using a Berendsen barostat with a time constant of 1 ps and a compressibility of 3 × 10^{-5}/bar, employing semi-isotropic pressure coupling to maintain constant pressure. Long-range electrostatics were calculated using the particle mesh ewald (PME) method,[36,37] with a relative dielectric constant of 2.5 and a cutoff distance of 1.6 nm. The Lennard−Jones interactions were modified according to the GROMACS Shift scheme, transitioning from 0.9 to 0 at 1.2 nm. Four independent replica simulations with a random set of initial velocities were performed for all of the simulation systems.

Analysis. Aβ_{16-22} peptide is classified as embedded/adsorbed within the lipid bilayer membrane if any of the terminal side chain (S2) beads of the phenylalanines (F19 and F20) are situated below the plane defined by six lipid phosphate groups nearest to the peptide.

Aβ_{16-22} aggregate is characterized as two or more peptides having at least 4 beads (out of 17 beads present in each peptide) within 0.7 nm. To quantify the alignment of peptides within each aggregate, we computed the nematic order parameter using the following formula:

$$P_2 = \frac{1}{2}(3\langle\cos^2(\theta)\rangle - 1)$$

where θ represents the angle between a peptide's end-to-end vector and the director vector. The end-to-end vector was defined using the backbone beads of residues K16 and E22, while the director vector indicates the direction of preferred alignment within the aggregate.[38]

A lipid cluster is characterized as a group of 3 or more lipids (with n_l denoting the number of lipids in the cluster) with PO4-PO4 contacts, defined using a cutoff distance of 0.9 nm. We calculated the adjacency ratio for each POPS lipid using voronoi tessellation. The adjacency ratio, r, for a given POPS lipid is defined as the number of POPS to POPC lipid neighbors. We calculated the distribution of n_l for clusters, both mediated and not mediated by peptides.

To quantify peptide interactions with the lipid bilayer, we analyze two key aspects: (1) the first interaction probability of peptides with different bilayer components (embedded peptides, POPS lipids, and POPC lipids, detailed below) and (2) the amino acid residue responsible for initial contact. To define a bilayer-peptide contact, we required at least 4 CG beads of the peptide to be within 0.7 nm of the bilayer components. For each peptide, we identify the frame of first contact, defined as the first instance where the peptide maintains continuous contact with the bilayer groups for 5 ns or longer.

At the frame of first contact, we used BB beads for peptides and PO4 beads for lipids to define interactions, applying the distance cutoff. We then determined whether the peptide interacted directly or as part of an aggregate. In both scenarios, we categorized interactions with the following groups: embedded peptides (Peptide-Seed), POPS lipid clusters with size 3 or greater (POPS ($n_l \geq 3$)) or size 2 or lesser (POPS ($n_l <$

https://doi.org/10.1021/acs.jpcb.4c05636
J. Phys. Chem. B 2024, 128, 10831−10840

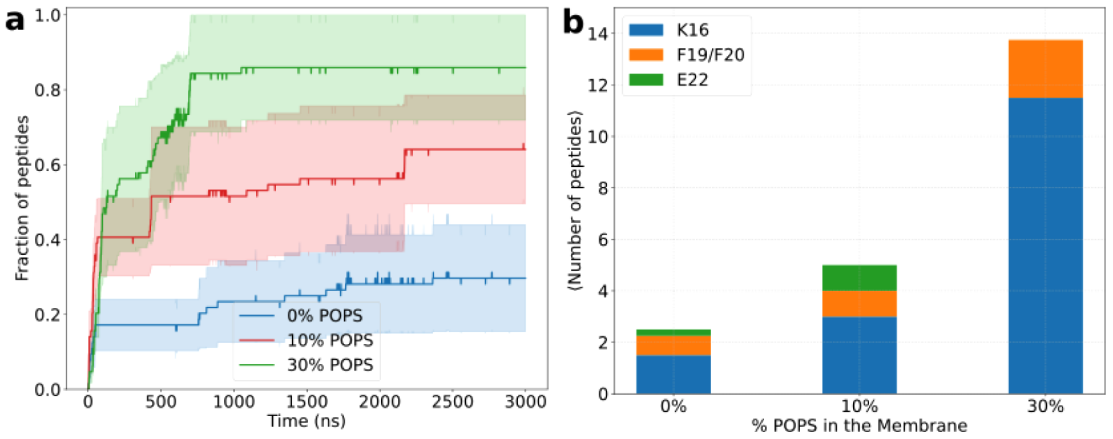

Figure 1. Aβ_{16-22} adsorption dynamics and initial interactions with lipid bilayers of varying POPS percentages. (a) Time evolution of the fraction of peptides adsorbed onto lipid bilayers containing 0%, 10%, and 30% POPS. Curves show averages of four simulations; shaded areas represent the standard error of the mean. (b) Average number of peptides interacting with the bilayer at the frame of first contact, categorized by amino acid type (positively charged, phenylalanine, and negatively charged) for different POPS percentages.

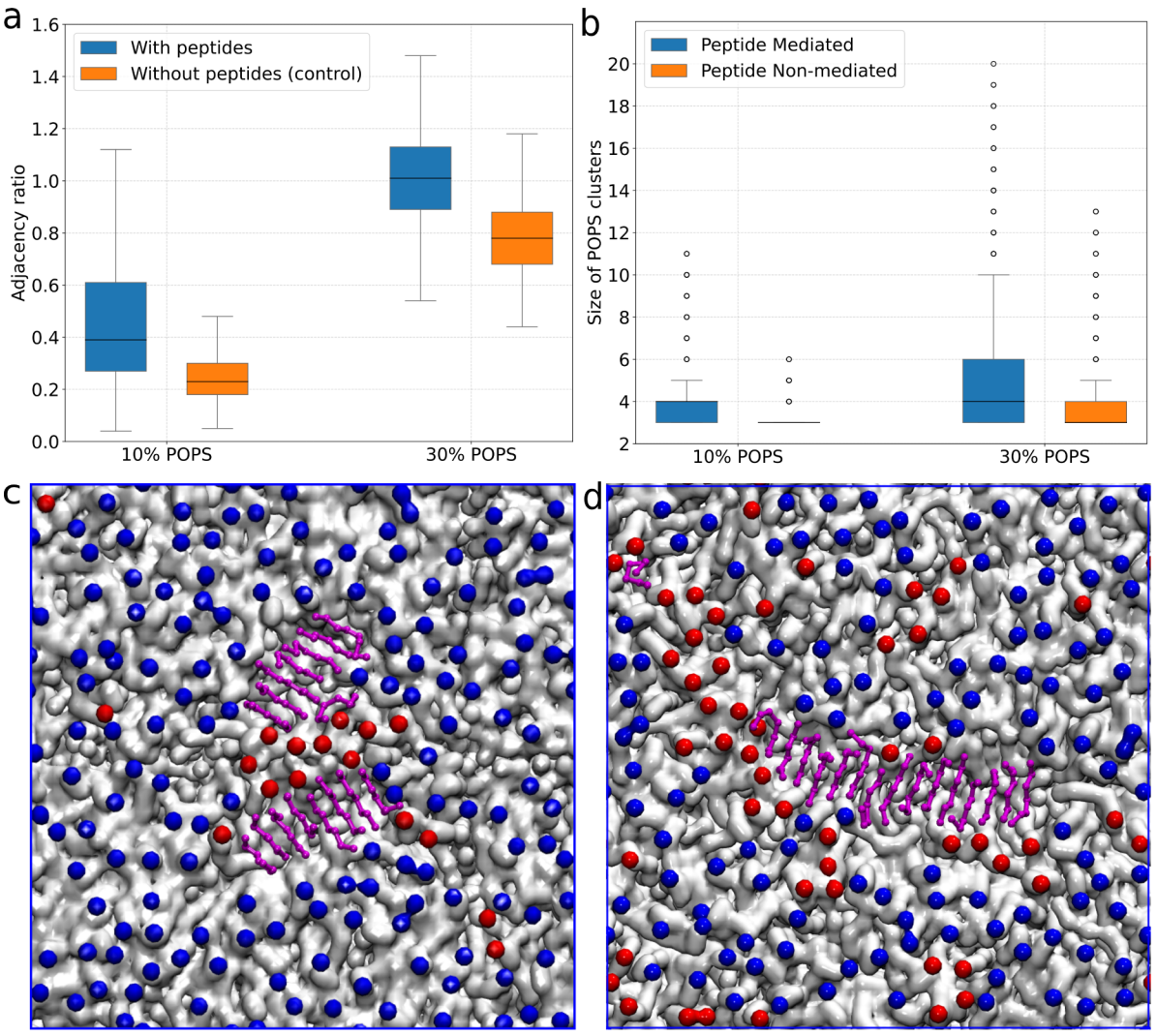

Figure 2. (a) Distribution of adjacency ratios for POPS lipids in 10% and 30% POPS bilayers with (blue) and without (orange) peptides. (b) Size distribution of POPS clusters mediated (blue) and not mediated (orange) by peptides in 10% and 30% POPS membranes. Representative snapshots illustrating POPS localization around peptide aggregates in (c) 10% and (d) 30% POPS bilayers. Color scheme: Peptide backbones (magenta), POPC phosphates (blue), POPS phosphates (red), lipid alkyl tails (white).

https://doi.org/10.1021/acs.jpcb.4c05636
J. Phys. Chem. B 2024, 128, 10831−10840

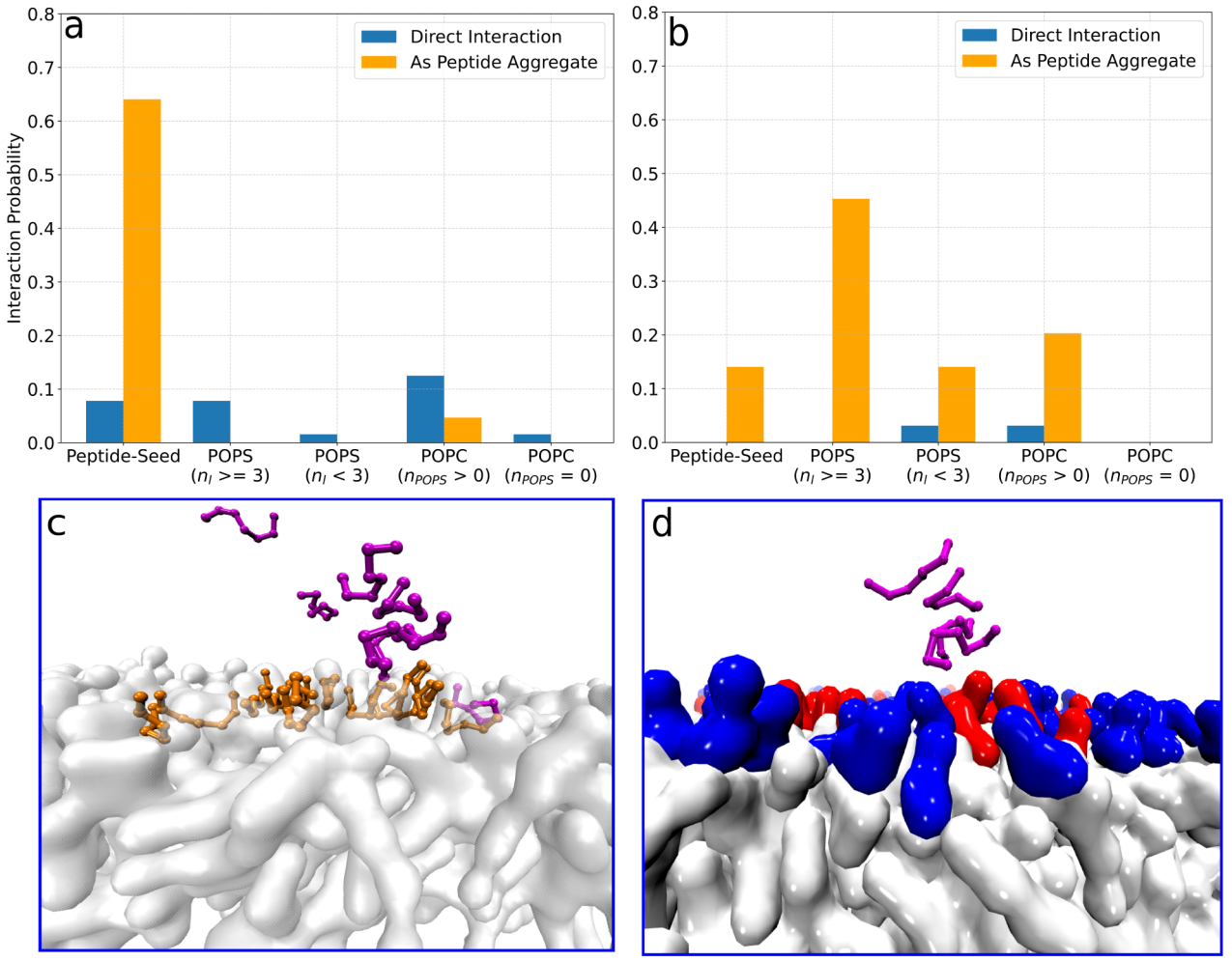

Figure 3. First interaction probabilities for Aβ_{16-22} peptides (a) with (extended simulations) and (b) without (original simulations) pre-existing peptides and aggregates on the bilayer. Snapshots showing peptide aggregate binding mediated by (c) peptide-seeds and (d) pops clusters for the extended simulation. Color scheme: Peptide aggregate backbones (magenta), peptide seed backbones (orange), POPC phosphates (blue), POPS phosphates (red), and lipid tails (white). Solvent particles, ions, dummy charges of BB beads, S1 and S2 side chain beads, and the lower leaflet are omitted for clarity.

3)), POPC lipids with (POPC (n_{POPS}> 0)) or without neighboring POPS molecules (POPC (n_{POPS}= 0)). When multiple groups interacted simultaneously, we identified the group nearest the BB beads as the primary contact point.

For peptides interacting directly or as aggregates with POPC or POPS lipids, we measured the distance between each amino acid's CG beads and the bilayer's PO4 beads. The amino acid with the shortest distance is designated as the initiator of the peptide's interaction with the bilayer.

Data analysis was conducted on the last 2000 ns of trajectories from four replica simulations per POPS percentage.

RESULTS

POPS-Enriched Membranes Enhance Peptide Adsorption and Interaction Kinetics. To investigate how the POPS enrichment in lipid bilayers affects peptide adsorption and interactions, we analyzed the fraction of peptides adsorbed on membranes with varying POPS percentages. Figure 1a shows the time evolution of this fraction's average, along with the standard error of the mean (SEM) for the four replicas. We observed that the presence of POPS in the mixed membranes enhances peptide/peptide aggregate adsorption onto them compared with pure POPC membranes. These findings align with atomic force microscopy (AFM) studies on zwitterionic (DOPC) and anionic (DOPG) lipid bilayers with Aβ_{1-42} peptide, which showed a similar trend, with DOPG bilayers exhibiting a higher volume of adsorbed peptide oligomers.[39]

To understand the role of lipid composition on peptide interactions with the bilayer, we analyzed the density distribution of key amino acid residues and phosphate groups in three different POPS bilayers (Figure S5). The analysis showed that the hydrophobic phenylalanine side chains go deeper into the bilayer as the POPS concentration increases compared to the charged residues. We observed an increase in the number density of CG beads of peptide residues with higher percentages of POPS, indicating enhanced peptide−lipid interactions in POPS-enriched bilayers.

This increased interaction can be attributed to two factors. First, stronger electrostatic interaction between the negatively charged POPS headgroups and positively charged amino acid of the peptides help anchor and retain peptides near the bilayer surface.[17] Second, the greater heterogeneity in membranes with higher POPS percentages creates more distinct low-lipid density regions (Figure S6), where peptides' hydrophobic residues can bind. Consequently, we observe an increase in the average number of peptides that initially interact with the bilayer

https://doi.org/10.1021/acs.jpcb.4c05636
J. Phys. Chem. B 2024, 128, 10831−10840

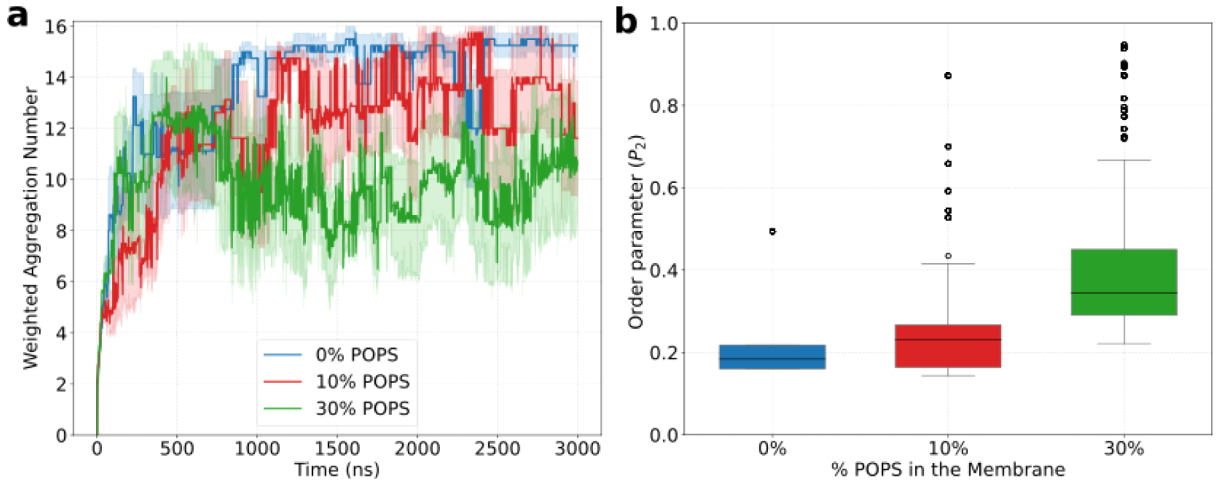

Figure 4. Aggregation dynamics of Aβ_{16-22} peptides with varying POPS membrane composition. (a) Time evolution of the weighted aggregation number for 0%, 10%, and 30% POPS membranes. Each curve shows the average of four independent simulations with shaded areas representing the standard error of the mean. (b) Distribution of order parameters for Aβ aggregates across different POPS percentages. Data is collected from the last 2000 ns of four simulations per condition.

through K16 and bulky hydrophobic residues (F19 and F20) for higher percentages of POPS, as shown in Figure 1b. In particular, there is a significant increase in the number of peptides that interact with lipids as POPS% increases, accompanied by a shift in the relative contributions of different amino acids at the frame of first contact (Figure 1b). The percentage of peptides interacting via K16 increases considerably (from 60% to 83.6%) for 30% POPS mixed membrane compared to pure POPC membrane, leading to a drop in the percentage of peptides interacting via other amino acids. This indicates a more dominant role of electrostatic interactions for peptide adsorption onto the bilayer. Our observation aligns with experimental studies that have demonstrated enhanced peptide adsorption to anionic lipid membranes due to electrostatic attraction between positively charged residues of peptides and negatively charged lipid headgroups.[40]

Peptides Enhance Lateral Heterogeneity in Membranes Containing POPS Lipids. Figure 2a shows the distribution of adjacency ratios (r) for POPS lipids, comparing systems with and without peptides (control) for both 10% and 30% POPS membranes. Simulations with peptides exhibit higher median adjacency ratios ($r = 0.39 \pm 0.26$ and 1.01 ± 0.18 for 10% and 30% POPS, respectively) compared to those without peptides ($r = 0.23 \pm 0.09$ and 0.78 ± 0.14 for 10% and 30% POPS, respectively). Higher r values for simulations with peptides demonstrate that Aβ_{16-22} binding enhances lipid demixing, leading to the formation of POPS-enriched clusters (regions of high negative charge density) on the bilayer. We calculated the proportion of the POPS: POPC lipid interactions with Aβ_{16-22} peptides by comparing the normalized number of contacts between Aβ_{16-22}−BB beads with lipid−PO4 beads. The contacts were calculated over the last 2000 ns for the 4 replicas of 30% PS and were normalized by the number of frames and lipid type. We obtained a mean ratio of 7.43 ± 1.35 for POPS−Aβ_{16-22} vs POPC−Aβ_{16-22}, which is significantly higher ($p < 0.001$, t test) than the expected no-preference value of 0.43, which represents the POPS:POPC ratio in the membrane. These results show the strong preference of Aβ_{16-22} peptides for POPS over that of POPC lipids. This preference leads to the formation of POPS clusters around Aβ_{16-22} aggregates bound to the lipid bilayer, a phenomenon visible in Figure 2c,d. This observation aligns with previous reports of accelerated lipid demixing in DPPG/DPPE mixed membranes, upon the binding of antimicrobial peptide, leading to two peaks in the DSC curve indicating DPPG- and DPPE-enriched domains.[41]

Figure 2b illustrates the distribution of POPS cluster sizes, both peptide-mediated and nonmediated. Peptide-mediated clusters show a median size of 4 with interquartile ranges (IQR) of 1.0 and 3.0 for 10% and 30% POPS, respectively. Nonmediated clusters have a median size of 3 with IQRs of 0.0 and 1.0 for 10% and 30% POPS, respectively. Higher IQRs are observed for peptide-mediated clusters because of the varied sizes of peptide aggregates bound to the lipid bilayer for PS containing membranes. This peptide-mediated lateral heterogeneity modifies the interaction of the membrane with the solution peptides (Figure 3a,b) and could lead to different mechanisms of membrane disruption, such as changes in the physiological properties of the membrane, carpeting and detergent effects.[42,43]

We analyzed membrane thickness changes in bilayers containing 0% and 30% POPS at the start and end of our simulations (Figure S7). For the 0% POPS bilayer, membrane thickness of 3.64 nm, similar to small unilamellar vesicles (SUVs) used in experiments,[44] decreased by 0.28 nm upon peptide interaction. 30% POPS bilayer showed similar thinning, from 3.51 to 3.27 nm. Although such peptide-induced membrane thinning is reported with all-atom simulations,[45] the magnitude of thinning in our study is less pronounced. This difference can be attributed to the use of a shorter peptide fragment (Aβ_{16-22}) as a representative model of the full-length Aβ peptide (similar to references[46−48]). This segment lacks the transmembrane domain (residues 29−42)[49] of Aβ peptide, due to which the peptide primarily interacts with the bilayer surface rather than deeply penetrating it (Figure S8).

Membrane-Bound Peptides Serve as Nucleation Seeds, Facilitating Aggregate Growth. To examine how embedded peptides influence interactions between solution peptides and the lipid bilayer, we extended the 30% POPS simulation by introducing 16 additional peptides into the final frame of the original run. This corresponds to a peptide concentration of ∼25.6 mM and a lipid:peptide ratio of ∼5:1. These 1000 ns simulations featured membranes with pre-

https://doi.org/10.1021/acs.jpcb.4c05636
J. Phys. Chem. B 2024, 128, 10831−10840

existing peptide aggregates. Figure 3 illustrates the first interaction probabilities for both extended (a) and original (b) simulations. The bar plots, averaged over four replicas per system, were generated by analyzing the frame of first contact for peptides using the protocol described in the analysis section. To differentiate between peptide-mediated and spontaneous lipid clusters, we categorized POPS lipids into two groups based on cluster size. As shown in Figure 2b, lipid clusters with $n_l \geq 3$ were predominantly peptide-mediated, while smaller clusters ($n_l < 3$) were likely to form spontaneously.

In the extended simulation, most of the peptides contacted the bilayer as aggregates interacting with the peptide seed (64%) or POPC lipids (5%). Other interaction modes included direct contact with POPC lipids (14%), peptide-seeds (8%), and POPS clusters (10%). Conversely, in the original run, peptides primarily contacted the bilayer as aggregates interacting through POPS clusters with $n_l \geq 3$ (45%) and $n_l < 3$ (14%), peptide-seed (14%), and POPC lipids (2%), with minimal direct interactions (6%).

The presence of embedded peptides in the bilayer accelerated the adsorption of solution peptides onto the bilayer (Figure S9) thereby increasing direct peptide−bilayer interactions, evidenced by a shift in direct interactions from 6% to 31%. This enhanced interaction may contribute to the increased cytotoxic effects of amyloid-beta at higher POPS percentages through mechanisms such as membrane thinning and increased permeability leading to ion dyshomeostasis.[10] Analysis of the first interaction probabilities (Figure 3) showed that binding of the peptide-aggregate to the bilayer occurred predominantly through two mechanisms: interaction with a pre-existing peptide seed (Figure 3c) or with a POPS cluster (Figure 3d). Interestingly, POPC lipids, which facilitated the initial contact between peptide aggregates and the bilayer, were in the proximity of one or more POPS lipids. This is evidenced by the very low first interaction probability for POPC lipids with no neighboring POPS ($n_{POPS} = 0$) and emphasizes the essential role of POPS in mediating peptide-bilayer interactions.

Higher POPS% Promotes Smaller and More Ordered Peptide Aggregates. We monitored the aggregation dynamics of Aβ_{16-22} peptides with varying POPS bilayers, as shown in Figure 4a, which illustrates the time evolution of the weighted aggregation number/size. Interestingly, the weighted aggregation number for peptides is smaller for mixed membranes compared with pure POPC membranes. In pure POPC systems, peptide aggregation occurs predominantly in solution, forming stable structures with tightly packed hydrophobic cores. These solution-formed aggregates can interact with the membrane through hydrophobic patches present on the bilayer or through peptide-seeds (Figure S10).

In mixed membranes, the aggregation process is more complex. Small oligomers form in solution and either remain anchored to the bilayer surface through a peptide seed (Figure 3c) or become embedded within it. This adsorption of the peptide aggregate is facilitated by interaction with PS clusters or via gradual loss of anchored peptides to the bilayer, as shown in Movie S1. Embedded aggregates are more susceptible to fragmentation due to the absence of a stable hydrophobic core and the "slicing" effect of PS lipids on disordered aggregate regions (Movie S2). This increased fragmentation contributes to the smaller aggregation number observed in mixed membranes.

Furthermore, aggregates formed in simulations with a higher PS% exhibit greater structural order (Figure 4b). In pure POPC systems, the absence of acidic lipids promotes amorphous aggregation[42] with tight hydrophobic cores that hinder rearrangement into ordered configurations, contrasting with the more structured aggregates observed in simulations with higher PS% content. In mixed membranes, as mentioned earlier, aggregate formation occurs both in solution and on the membrane surface with membrane-bound aggregates predominantly surrounded by POPS lipids. The presence of POPS lipids impart structural order to the peptide aggregate through a templated ordering effect, as reported by Chi et al.[50]

These differences in aggregation behavior highlight how inclusion of PS in membranes affects the size and structure of the oligomers.

DISCUSSION

Lipid demixing, a natural process in biological membranes, involves the formation of domains or clusters of specific lipids, leading to heterogeneity in plasma membranes. Although this process has been reported to occur spontaneously in cells,[51] the binding of certain proteins can accelerate lipid demixing in mixed membranes containing acidic lipids,[52] leading to alteration in membrane structure and function.[29] This phenomenon has been observed in various studies, particularly for the formation of large PS domains induced by binding of peripheral proteins to mixed membrane systems.[53] Heimburg et al. demonstrated a notable example with cytochrome C: its binding to mixed anionic/zwitterionic membranes triggers lipid demixing, which in turn enhances further cytochrome C binding, illustrating a cooperative protein−lipid interaction. They also revealed a preferential clustering of anionic lipids around the bound protein.[53] Similar preferential interactions have been reported for other peptides, such as the preference of pentalysine for PS over PC[54] and the preference of cardiotoxin II for phosphatidylglycerol (PG) over PC.[55]

Our simulations of Aβ_{16-22} with mixed membranes support these findings. We observed increased adjacency ratios for POPS lipids in simulations containing peptides (Figure 2a), indicating that peptide binding promotes lipid demixing in the bilayer. This demixing process can be conceptualized as a balance between the adsorption energy gained from PS−Aβ_{16-22} interactions and the mixing entropy lost from the rearrangement of the PS lipids.[56] Consequently, large peptide-mediated PS clusters or regions of high negative charge density form on the bilayer (Figure 2b).

The lateral segregation of lipids in mixed membranes arises from the stronger electrostatic attractions between PC−PC and PS−PS pairs compared to mixed pairs.[19] Notably, cluster formation occurs predominantly among PS lipids due to their more robust headgroup interactions. Zak et al. report that the electrostatic attraction between PS lipids is nearly twice that of PC lipids.[19] Our simulations corroborate these findings, revealing a preference for PS−PS interactions over PS−PC interactions. This preference is evident even in peptide-free systems, where the median adjacency ratios observed for POPS lipids (0.23 and 0.78 for 10% PS and 30% PS systems, respectively) exceed the theoretical value (0.11 and 0.43) expected for a random distribution. The strong PS−PS headgroup interactions stem from dipole−dipole interactions between the CNO beads (serine headgroups) of POPS lipids.[19] Aβ_{16-22}'s preferential interaction with POPS over POPC, due to dipole interactions between the peptide backbone and POPS serine headgroups, leads to the clustering of PS lipids around peptide aggregates bound to the bilayer. This clustering further enhances the adjacency ratios for PS lipids, exceeding the values

https://doi.org/10.1021/acs.jpcb.4c05636
J. Phys. Chem. B 2024, 128, 10831−10840

observed in peptide-free systems, as seen in Figure 2a. These peptide−lipid clusters not only alter the physiological properties of the bilayer[42,43] but also accelerate the adsorption of solution peptides onto the bilayer (Figure S9). This demonstrates a cooperative effect in the binding of $A\beta_{16-22}$ to the bilayer, highlighting the complex interplay between peptide aggregation and lipid organization in membrane systems.

Our simulations employ higher than physiological levels of $A\beta_{16-22}$, a common approach in the MD community, to reduce diffusion-controlled protein encounter times in computer simulations.[57−60] As previously noted, conflicting results exist regarding the impact of anionic lipid composition on the aggregation kinetics of neurodegenerative peptides. We propose that the net effect depends on a balance between two competing factors: (a) acceleration due to increased peptide concentration at anionic membrane interfaces,[7] and (b) deceleration caused by PS lipids that inhibit peptide aggregate growth by screening peptide−peptide interactions on the membrane surface.[17]

The concentration of the peptide influences the interplay between these factors. In the lower concentration regime of $A\beta$, where most peptides adsorb onto the bilayer as monomers, anionic lipids tend to decelerate aggregation kinetics by inhibiting the growth of peptide aggregates (Figure S12) on the membrane surface. In contrast, in concentrated $A\beta$ solutions, where aggregation occurs primarily in solution, anionic lipids facilitate the adsorption of peptide aggregates (Figure 3d), creating nucleation seeds on the bilayer. These seeds facilitate the perpendicular growth of aggregates from the bilayer surface (Figure S11), thus accelerating the aggregation kinetics. This concentration-dependent behavior reconciles contradictory observations in the literature and highlights the complexity of the amyloid aggregation processes in mixed lipid membranes.

The Movie S2 illustrates PS lipids not only interposing between peptides but also cleaving disordered peptides from the peptide aggregate. Consequently, membranes containing PS lipids exhibit smaller, more ordered aggregates (Figure 4). These small aggregates create more peptide seeds on the bilayer, accelerating peptide−bilayer interactions and demonstrating a cooperative effect in $A\beta_{16-22}$ binding.

CONCLUSION

Our results show the effects of the inclusion of PS lipids on $A\beta_{16-22}$ adsorption kinetics and aggregation behavior. We observe enhanced adsorption of $A\beta_{16-22}$ peptides with PS/PC mixed membranes, primarily driven by electrostatics. We also see distinct aggregation patterns depending on membrane composition. Pure POPC membranes foster the formation of large, amorphous aggregates in solution, characterized by tightly packed hydrophobic residues resistant to rearrangement. These aggregates can interact with the membrane through peptide-seeds or hydrophobic patches present on the bilayer. In contrast, mixed PS/PC membranes promote rapid adsorption of solution-formed oligomers, a process facilitated by PS lipids or pre-existing peptide seeds. The templating effect of PS lipids confer order to these bilayer-adsorbed aggregates. Furthermore, PS lipids inhibit the growth of peptide aggregates by screening peptide−peptide interactions, leading to small ordered fragments. These fragments serve as nucleation seeds, accelerating the adsorption of solution peptides onto the bilayer and facilitating the growth of peptide aggregates perpendicular to the membrane. Thus, anionic lipids play a dual role in the aggregation of $A\beta_{16-22}$. They modulate the aggregation kinetics, with the net effect depending on the concentration of peptides in the solution. Our simulations also demonstrate that the binding of the $A\beta_{16-22}$ peptide induces lipid demixing, resulting in the formation of large, peptide-mediated PS clusters on the bilayer. These clusters disrupt lateral homogeneity and enhance peptide−membrane interactions. This work provides crucial insights into the multifaceted roles of anionic lipids in modulating the adsorption and aggregation behavior of amyloid peptides. By delineating these complex interactions, our study contributes to a more nuanced understanding of membrane-mediated peptide aggregation in neurodegenerative disorders, potentially guiding new therapeutic strategies targeting early stages of protein aggregation in various neurodegenerative diseases.

ASSOCIATED CONTENT

Data Availability Statement

All files that are required to set up and perform the simulations described in this work can be found at https://github.com/meenaljainumd/PCPS_amyloid_aggregation. The molecular trajectories and the portable binary run input file used in this article can be found at 10.5281/zenodo.13288435.

Supporting Information

The Supporting Information is available free of charge at https://pubs.acs.org/doi/10.1021/acs.jpcb.4c05636.

Schematic representations of coarse-grained (CG) amino-acids and lipid models (POPC and POPS); CG bead types present in $A\beta$16−22 fragment, lipid molecules and MARTINI-polarizable solvent; nonbonded interaction parameters for main and dummy bead types; area-per-lipid vs surface tension (ST) plots for various POPS concentrations; simulation protocol for surface tension determination at different POPS percentages; surface tension values corresponding to POPS concentrations; lipid density contours illustrating membrane heterogeneity; evolution of fraction of peptides interacting with the bilayer for extended and original simulations (PDF)

POPS lipids (red) infiltrate and cleave disordered peptides from a peptide aggregate (magenta). Color scheme: Peptide backbones (magenta), POPS:PO4 (red), POPC:PO4 and lipid alkyl tails (white) (MOV)

Time-lapse visualization of peptide dissociation from an anchored aggregate into a lipid bilayer. Color scheme: Peptide backbones (magenta), POPC phosphates (blue), POPS phosphates (red), lipid alkyl tails (white) (MP4)

AUTHOR INFORMATION

Corresponding Author

Silvina Matysiak − *Department of Chemistry and Biochemistry and Fischell Department of Bioengineering, University of Maryland, College Park, Maryland 20742, United States;* orcid.org/0000-0003-3824-9787; Phone: +1 301-405-0313; Email: matysiak@umd.edu

Author

Meenal Jain − *Department of Chemistry and Biochemistry, University of Maryland, College Park, Maryland 20742, United States*

Complete contact information is available at: https://pubs.acs.org/10.1021/acs.jpcb.4c05636

Notes

The authors declare no competing financial interest.

https://doi.org/10.1021/acs.jpcb.4c05636
J. Phys. Chem. B 2024, 128, 10831−10840

■ ACKNOWLEDGMENTS

We acknowledge the financial support from the National Science Foundation under grant CHE-2202281 and computational resources at the University of Maryland. M.J. would like to thank Suhas Gotla for providing the order parameter code and for assistance with the simulation analysis. The author also thanks Abhilash Sahoo, Neha Nanajkar, Jessica Bodosa, and Riya Samanta for discussions and insightful suggestions.

■ REFERENCES

(1) Ke, P. C.; Sani, M.-A.; Ding, F.; Kakinen, A.; Javed, I.; Separovic, F.; Davis, T. P.; Mezzenga, R. Implications of peptide assemblies in amyloid diseases. *Chem. Soc. Rev.* **2017**, *46*, 6492−6531.
(2) Hampel, H.; Hardy, J.; Blennow, K.; Chen, C.; Perry, G.; Kim, S. H.; Villemagne, V. L.; Aisen, P.; Vendruscolo, M.; Iwatsubo, T. The amyloid-β pathway in Alzheimer's disease. *Mol. Psychiatry* **2021**, *26*, 5481−5503.
(3) Verma, M.; Vats, A.; Taneja, V. Toxic species in amyloid disorders: Oligomers or mature fibrils. *Ann. Indian Acad. Neurol.* **2015**, *18*, 138−145.
(4) Viles, J. H. Imaging Amyloid-β Membrane Interactions: Ion-Channel Pores and Lipid-Bilayer Permeability in Alzheimer's Disease. *Angew. Chem., Int. Ed.* **2023**, *62*, No. e202215785.
(5) Sabaté, R.; Espargaró, A.; Barbosa-Barros, L.; Ventura, S.; Estelrich, J. Effect of the surface charge of artificial model membranes on the aggregation of amyloid β-peptide. *Biochimie* **2012**, *94*, 1730−1738.
(6) Sanguanini, M.; Baumann, K. N.; Preet, S.; Chia, S.; Habchi, J.; Knowles, T. P.; Vendruscolo, M. Complexity in lipid membrane composition induces resilience to Aβ42 aggregation. *ACS Chem. Neurosci.* **2020**, *11*, 1347−1352.
(7) Niu, Z.; Zhao, W.; Zhang, Z.; Xiao, F.; Tang, X.; Yang, J. The Molecular Structure of Alzheimer β-Amyloid Fibrils Formed in the Presence of Phospholipid Vesicles. *Angew. Chem.* **2014**, *126*, 9448−9451.
(8) Lv, Z.; Hashemi, M.; Banerjee, S.; Zagorski, K.; Rochet, J.-C.; Lyubchenko, Y. L. Assembly of α-synuclein aggregates on phospholipid bilayers. *Biochim. Biophys. Acta, Proteins Proteomics* **2019**, *1867*, 802−812.
(9) Andrade, S.; Loureiro, J. A.; Pereira, M. C. The Role of Amyloid β-Biomembrane Interactions in the Pathogenesis of Alzheimer's Disease: Insights from Liposomes as Membrane Models. *ChemPhyschem* **2021**, *22*, 1547−1565.
(10) Butterfield, S. M.; Lashuel, H. A. Amyloidogenic protein−membrane interactions: Mechanistic insight from model systems. *Angew. Chem., Int. Ed.* **2010**, *49*, 5628−5654.
(11) Kayed, R.; Head, E.; Thompson, J. L.; McIntire, T. M.; Milton, S. C.; Cotman, C. W.; Glabe, C. G. Common structure of soluble amyloid oligomers implies common mechanism of pathogenesis. *Science* **2003**, *300*, 486−489.
(12) Das, P.; Matysiak, S.; Mittal, J. Looking at the disordered proteins through the computational microscope. *ACS Cent. Sci.* **2018**, *4*, 534−542.
(13) Kmiecik, S.; Gront, D.; Kolinski, M.; Wieteska, L.; Dawid, A. E.; Kolinski, A. Coarse-grained protein models and their applications. *Chem. Rev.* **2016**, *116*, 7898−7936.
(14) Harayama, T.; Riezman, H. Understanding the diversity of membrane lipid composition. *Nat. Rev. Mol. Cell Biol.* **2018**, *19*, 281−296.
(15) Leventis, P. A.; Grinstein, S. The distribution and function of phosphatidylserine in cellular membranes. *Annu. Rev. Biophys.* **2010**, *39*, 407−427.
(16) Ali, A.; Dou, T.; Holman, A. P.; Hung, A.; Osborne, L.; Pickett, D.; Rodriguez, A.; Zhaliazka, K.; Kurouski, D. The influence of Zwitterionic and anionic phospholipids on protein aggregation. *Biophys. Chem.* **2024**, *306*, 107174.
(17) Sahoo, A.; Xu, H.; Matysiak, S. Pathways of amyloid-beta absorption and aggregation in a membranous environment. *Phys. Chem. Chem. Phys.* **2019**, *21*, 8559−8568.
(18) Jurkiewicz, P.; Cwiklik, L.; Vojtíšková, A.; Jungwirth, P.; Hof, M. Structure, dynamics, and hydration of POPC/POPS bilayers suspended in NaCl, KCl, and CsCl solutions. *Biochim. Biophys. Acta, Biomembr.* **2012**, *1818*, 609−616.
(19) Zak, A.; Korshunova, K.; Rajtar, N.; Kulig, W.; Kepczynski, M. Deciphering Lipid Arrangement in Phosphatidylserine/Phosphatidylcholine Mixed Membranes: Simulations and Experiments. *Langmuir* **2023**, *39*, 18995−19007.
(20) Balbach, J. J.; Ishii, Y.; Antzutkin, O. N.; Leapman, R. D.; Rizzo, N. W.; Dyda, F.; Reed, J.; Tycko, R. Amyloid fibril formation by Aβ16−22, a seven-residue fragment of the Alzheimer's β-amyloid peptide, and structural characterization by solid state NMR. *Biochemistry* **2000**, *39*, 13748−13759.
(21) Sureshbabu, N.; Kirubagaran, R.; Thangarajah, H.; Malar, E. P.; Jayakumar, R. Lipid-induced conformational transition of amyloid β peptide fragments. *J. Mol. Neurosci.* **2010**, *41*, 368−382.
(22) Ganesan, S. J.; Matysiak, S. Role of Backbone Dipole Interactions in the Formation of Secondary and Supersecondary Structures of Proteins. *J. Chem. Theory Comput.* **2014**, *10*, 2569−2576.
(23) Ganesan, S. J.; Xu, H.; Matysiak, S. Effect of lipid head group interactions on membrane properties and membrane-induced cationic β-hairpin folding. *Phys. Chem. Chem. Phys.* **2016**, *18*, 17836−17850.
(24) Yesylevskyy, S. O.; Schäfer, L. V.; Sengupta, D.; Marrink, S. J. Polarizable water model for the coarse-grained MARTINI force field. *PloS Comput. Biol.* **2010**, *6*, No. e1000810.
(25) Banerjee, S.; Hashemi, M.; Zagorski, K.; Lyubchenko, Y. L. Interaction of Aβ42 with membranes triggers the self-assembly into oligomers. *Int. J. Mol. Sci.* **2020**, *21*, 1129.
(26) Ganesan, S. J.; Matysiak, S. Interplay between the hydrophobic effect and dipole interactions in peptide aggregation at interfaces. *Phys. Chem. Chem. Phys.* **2016**, *18*, 2449−2458.
(27) Jain, M.; Sahoo, A.; Matysiak, S. Modulation of Aβ 16−22 aggregation by glucose. *Phys. Chem. Chem. Phys.* **2024**, *26*, 5038−5044.
(28) Gotla, S.; Matysiak, S. Mechanistic insights into the inhibition of amyloid-β aggregation by chitosan. *Phys. Chem. Chem. Phys.* **2023**, *25*, 10113−10120.
(29) Sahoo, A.; Matysiak, S. A Microscopic Picture of Calcium-Assisted Lipid Demixing and Membrane Remodeling using Multi-Scale Simulations. *Biophys. J.* **2020**, *118*, 83a−84a.
(30) Sahoo, A.; Matysiak, S. Effects of applied surface-tension on membrane-assisted Aβ aggregation. *Phys. Chem. Chem. Phys.* **2021**, *23*, 20627−20633.
(31) Marrink, S. J.; Risselada, H. J.; Yefimov, S.; Tieleman, D. P.; de Vries, A. H. The MARTINI Force Field: Coarse Grained Model for Biomolecular Simulations. *J. Phys. Chem. B* **2007**, *111*, 7812−7824.
(32) de Jong, D. H.; Singh, G.; Bennett, W. F. D.; Arnarez, C.; Wassenaar, T. A.; Schäfer, L. V.; Periole, X.; Tieleman, D. P.; Marrink, S. J. Improved Parameters for the MARTINI Coarse-Grained Protein Force Field. *J. Chem. Theory Comput.* **2013**, *9*, 687−697.
(33) Wassenaar, T. A.; Ingólfsson, H. I.; Bockmann, R. A.; Tieleman, D. P.; Marrink, S. J. Computational lipidomics with insane: A versatile tool for generating custom membranes for molecular simulations. *J. Chem. Theory Comput.* **2015**, *11*, 2144−2155.
(34) Kandel, N.; Zheng, T.; Huo, Q.; Tatulian, S. A. Membrane binding and pore formation by a cytotoxic fragment of amyloid β peptide. *J. Phys. Chem. B* **2017**, *121*, 10293−10305.
(35) Nosé, S. A molecular dynamics method for simulations in the canonical ensemble. *Mol. Phys.* **1984**, *52*, 255−268.
(36) Darden, T.; York, D.; Pedersen, L. Particle mesh Ewald: An N.log(N) method for Ewald sums in large systems. *J. Chem. Phys.* **1993**, *98*, 10089−10092.
(37) Essmann, U.; Perera, L.; Berkowitz, M. L.; Darden, T.; Lee, H.; Pedersen, L. G. A smooth particle mesh Ewald method. *J. Chem. Phys.* **1995**, *103*, 8577−8593.

https://doi.org/10.1021/acs.jpcb.4c05636
J. Phys. Chem. B 2024, 128, 10831−10840

(38) Cecchini, M.; Rao, F.; Seeber, M.; Caflisch, A. Replica exchange molecular dynamics simulations of amyloid peptide aggregation. *J. Chem. Phys.* **2004**, *121*, 10748−10756.
(39) Hane, F.; Drolle, E.; Gaikwad, R.; Faught, E.; Leonenko, Z. Amyloid-β aggregation on model lipid membranes: An atomic force microscopy study. *J. Alzheimers Dis.* **2011**, *26*, 485−494.
(40) McLaurin, J.; Chakrabartty, A. Characterization of the interactions of Alzheimer β-amyloid peptides with phospholipid membranes. *Eur. J. Biochem.* **1997**, *245*, 355−363.
(41) Arouri, A.; Dathe, M.; Blume, A. Peptide induced demixing in PG/PE lipid mixtures: A mechanism for the specificity of antimicrobial peptides towards bacterial membranes? *Biochim. Biophys. Acta, Biomembr.* **2009**, *1788*, 650−659.
(42) Yip, C. M.; McLaurin, J. Amyloid-ß Peptide Assembly: A Critical Step in Fibrillogenesis and Membrane Disruption. *Biophys. J.* **2001**, *80*, 1359−1371.
(43) Bokvist, M.; Lindström, F.; Watts, A.; Gröbner, G. Two types of Alzheimer's β-amyloid (1−40) peptide membrane interactions: Aggregation preventing transmembrane anchoring versus accelerated surface fibril formation. *J. Mol. Biol.* **2004**, *335*, 1039−1049.
(44) Rex, S. Pore formation induced by the peptide melittin in different lipid vesicle membranes. *Biophys. Chem.* **1996**, *58*, 75−85.
(45) Grasso, G.; Lionello, C.; Stojceski, F. Highlighting the effect of amyloid beta assemblies on the mechanical properties and conformational stability of cell membrane. *J. Mol. Graphics Modell.* **2020**, *100*, 107670.
(46) Dasari, S.; Mallik, B. S. Conformational dynamics of amyloid-β (16−22) peptide in aqueous ionic liquids. *RSC Adv.* **2020**, *10*, 33248−33260.
(47) Pal, S.; Paul, S. ATP Controls the aggregation of Aβ16−22 peptides. *J. Phys. Chem. B* **2020**, *124*, 210−223.
(48) Latshaw, D. C.; Cheon, M.; Hall, C. K. Effects of macromolecular crowding on amyloid beta (16−22) aggregation using coarse-grained simulations. *J. Phys. Chem. B* **2014**, *118*, 13513−13526.
(49) Millucci, L.; Ghezzi, L.; Bernardini, G.; Santucci, A. Conformations and biological activities of amyloid beta peptide 25−35. *Curr. Protein Pept. Sci.* **2010**, *11*, 54−67.
(50) Chi, E. Y.; Ege, C.; Winans, A.; Majewski, J.; Wu, G.; Kjaer, K.; Lee, K. Y. C. Lipid membrane templates the ordering and induces the fibrillogenesis of Alzheimer's disease amyloid-β peptide. *Proteins* **2008**, *72*, 1−24.
(51) Bagatolli, L. A.; Ipsen, J. H.; Simonsen, A. C.; Mouritsen, O. G. An outlook on organization of lipids in membranes: Searching for a realistic connection with the organization of biological membranes. *Prog. Lipid Res.* **2010**, *49*, 378−389.
(52) Sankaram, M. B.; Marsh, D. *New Comprehensive Biochemistry*; Elsevier: Amsterdam, 1993; Vol. *25*, pp. 127−162.
(53) Heimburg, T.; Angerstein, B.; Marsh, D. Binding of peripheral proteins to mixed lipid membranes: Effect of lipid demixing upon binding. *Biophys. J.* **1999**, *76*, 2575−2586.
(54) Roux, M.; Neumann, J.-M.; Bloom, M.; Devaux, P. F. 2H and 31 P NMR study of pentalysine interaction with headgroup deuterated phosphatidylcholine and phosphatidylserine. *Eur. Biophys. J.* **1988**, *16*, 267−273.
(55) Carbone, M. A.; Macdonald, P. M. Cardiotoxin II segregates phosphatidylglycerol from mixtures with phosphatidylcholine: 31P and 2H NMR spectroscopic evidence. *Biochemistry* **1996**, *35*, 3368−3378.
(56) May, S.; Harries, D.; Ben-Shaul, A. Lipid demixing and protein-protein interactions in the adsorption of charged proteins on mixed membranes. *Biophys. J.* **2000**, *79*, 1747−1760.
(57) Carballo-Pacheco, M.; Ismail, A. E.; Strodel, B. Oligomer Formation of Toxic and Functional Amyloid Peptides Studied with Atomistic Simulations. *J. Phys. Chem. B* **2015**, *119*, 9696−9705.
(58) Matthes, D.; Gapsys, V.; Daebel, V.; de Groot, B. L. Mapping the Conformational Dynamics and Pathways of Spontaneous Steric Zipper Peptide Oligomerization. *PLoS One* **2011**, *6*, No. e19129.
(59) Barz, B.; Wales, D. J.; Strodel, B. A Kinetic Approach to the Sequence−Aggregation Relationship in Disease-Related Protein Assembly. *J. Phys. Chem. B* **2014**, *118*, 1003−1011.
(60) Matthes, D.; Gapsys, V.; de Groot, B. L. Driving Forces and Structural Determinants of Steric Zipper Peptide Oligomer Formation Elucidated by Atomistic Simulations. *J. Mol. Biol.* **2012**, *421*, 390−416.

https://doi.org/10.1021/acs.jpcb.4c05636
J. Phys. Chem. B 2024, 128, 10831−10840